Development 138, 2925-2934 (2011) doi:10.1242/dev.065888

Sector analysis and predictive modelling reveal iterative shoot-like development in fern fronds

Heather L. Sanders, Peter R. Darrah and Jane A. Langdale*

SUMMARY

Plants colonized the terrestrial environment over 450 million years ago. Since then, shoot architecture has evolved in response to changing environmental conditions. Our current understanding of the innovations that altered shoot morphology is underpinned by developmental studies in a number of plant groups. However, the least is known about mechanisms that operate in ferns – a key group for understanding the evolution of plant development. Using a novel combination of sector analysis, conditional probability modelling methods and histology, we show that shoots, fronds ('leaves') and pinnae ('leaflets') of the fern *Nephrolepis exaltata* all develop from single apical initial cells. Shoot initials cleave on three faces to produce a pool of cells from which individual frond apical initials are sequentially specified. Frond initials then cleave in two planes to produce a series of lateral merophyte initials that each contributes a unit of three pinnae to half of the mediolateral frond axis. Notably, this iterative pattern in both shoots and fronds is similar to the developmental process that operates in shoots of other plant groups. Pinnae initials first cleave in two planes to generate lateral marginal initials. The apical and marginal initials then divide in three planes to coordinately generate the determinate pinna. These findings impact both on our understanding of fundamental plant developmental processes and on our perspective of how shoot systems evolved.

KEY WORDS: Sector analysis, Predictive modelling, Apical cells, Comparative development

INTRODUCTION

Shoot architecture varies both between and among land plant groups, with the observed differences resulting from varying contributions of indeterminate and determinate growth processes (for a review, see Steeves and Sussex, 1989). In most plants, shoot apical meristems develop indeterminately, whereas lateral organs develop in a determinate manner. Exceptions to this rule exist, for example, in annual plants, where the meristem terminates in a flower. However, even then there is an extended period of iterative apical growth where the meristem repeatedly generates equivalent structural units that together comprise the shoot. Iterative shoot development has been reported across the land plants, in both haploid gametophyte and diploid sporophyte generations. For example, a single apical initial generates repeating 'leaf' units in *Physcomitrella patens* gametophytes (Harrison et al., 2009), and in the lycophyte *Selaginella kraussiana*, one or two apical initials generate repeating units of leaf pairs along the bifurcating sporophyte stem (Harrison and Langdale, 2010; Harrison et al., 2007; Jones and Drinnan, 2009). In seed plants, iterative shoot development involves the repeated production of phytomer units from multicellular apical meristems (for a review, see Steeves and Sussex, 1989). Phytomers comprise a leaf, internode and axillary meristem (Galinat, 1959), and whether or not axillary meristems grow out to form branches determines the final architecture.

The evolution of leafy branched shoots can be traced in the fossil record, where it appears that early vascular plants had leafless dichotomously branching axes and that leaves evolved independently in lycophytes, monilophytes (ferns and horsetails) and seed plants (Kenrick and Crane, 1997). Enation (Bower, 1935), sporangium sterilization (Crane and Kenrick, 1997) and branch reduction (Zimmermann, 1952) theories of lycophyte leaf evolution have been proposed and recent studies have argued for (Harrison et al., 2005; Prigge and Clarke, 2006) and against (Floyd and Bowman, 2006) the parallel recruitment of similar genetic pathways in lycophytes and seed plants. In monilophytes, leaves probably evolved from regions of branched axes, as in seed plants (Zimmermann, 1952). However, both fossil evidence and gene expression patterns suggest that different mechanisms were adopted in the two groups (Sanders et al., 2009; Sano et al., 2005). A more coherent view of leaf evolution requires a rationalization of these apparent conflicts and such rationalization requires a better understanding of shoot development in monilophytes.

In the late 19th century, a number of reports suggested that fern shoots develop from a single apical initial cell (Bower, 1884; Hofmeister, 1857; Kny, 1875). However, these carefully documented studies were questioned in the mid-20th century when 'modern' histological techniques facilitated tissue sectioning. For 30 years, debates ensued about the existence, number and role of apical initial(s), and about the role of zonation within the apex (for a review, see White and Turner, 1995). The current consensus is that fern shoots, fronds and pinnae develop from one or two apical initials, with the actual number varying between species (Bierhorst, 1977; Hill, 2001; Pray, 1960). This consensus is derived from the examination of cleared shoot apices, histological sections and sequential surface imprints. Importantly, although each of these methods has merit, none has been used to examine the activity of shoot, frond and pinna initials in a single species.

Here, we have combined sector analysis of variegated *Nephrolepis exaltata* cv. *bostonensis* with histological information and conditional probability modelling, to provide a robust analysis of cell lineage patterns in a fern. Despite previous suggestions that

Department of Plant Sciences, University of Oxford, South Parks Road, Oxford OX1 3RB, UK.

*Author for correspondence (jane.langdale@plants.ox.ac.uk)

Accepted 6 May 2011

sectorial chimaeras cannot occur in ferns because shoot growth occurs from a single apical initial (Bierhorst, 1977), we confirm that shoots, fronds and pinnae of *N. exaltata* each develop from single initials. We further demonstrate that shoots and fronds develop iteratively, whereas pinnae are determinate. These findings are discussed in the context of our fundamental understanding of plant development and of land plant evolution.

MATERIALS AND METHODS

Plant material

Variegated *Nephrolepis exaltata* was obtained from Tropiflora Nurseries, Florida and non-variegated plants were obtained from garden centres in Oxford, UK. Plants were grown in the greenhouse on peat-based compost supplemented with slow-release fertilizer, under a diurnal light regime (16 hours light; 8 hours dark).

Histology and SEM

Plants were fixed in FAA (50% ethanol, 3.7% formaldehyde, 5% acetic acid), dehydrated and embedded in Paraplast Plus as described by the manufacturer (Paraplast, Leica). Eight or 10 μm sections were cut and stained with Toluidine Blue or Safranin O/Fast Green as described by Berlyn and Miksche (Berlyn and Miksche, 1976). For images of the crosier apex, samples were first embedded in polyoxsilane dental moulding material (Parkell). Plant material was then removed and replaced with Taab resin. Replicas were transferred to viewing stubs, coated and viewed in the SEM (JEOL JSM-5510).

Chlorophyll fluorescence

Pinnae samples (~2 mm^2) were soaked in 1% calcofluor white (1 hour under vacuum), washed twice in water and then viewed by confocal microscopy (Zeiss LSM 510). Epidermal peels were mounted in either water or 0.1% calcofluor and viewed by light (Olympus BX50) or confocal microscopy, respectively. Chlorophyll autofluorescence and calcofluor cell wall staining were detected using the 408 laser line with a 650 long pass emission (chorophyll) or a 515-530 band pass (calcofluor) filter. Shoot apex diagrams were generated using Googlesketchup 3D.

Characterization of frond sectors

One-hundred and fourteen fronds comprising 7160 pinnae were sampled randomly and photographed. Sector sizes were quantified by counting the number of pinnae comprising the sector. Sector position was recorded in the context of both proximodistal and mediolateral axes. Rachis sectors were examined using a hand lens or dissecting microscope.

Characterization of pinnae sectors

Pinnae sectors were quantified using image-processing software created in MATLAB. Pinnae from 14 randomly sampled fronds were scanned using a flat-bed scanner. Sectors were outlined manually to delineate green from yellow. Only sectors that extended from midvein to margin were analysed. These sectors were characterized by breadth at the midvein, rather than area, as the latter was overly biased by leaf shape. Sectors that did not extend from the midvein to margin normally occupied less than 1% of the total pinna area and encompassed a subset of epidermal and/or mesophyll cell layers. These sectors represented late cell division events and were not generally included in our analysis.

Formally, large sectors could arise by single mutations early in pinna development or by mutations in two adjacent cells later in development. If the former hypothesis is correct, large sectors would be half as common as sectors half their size. By contrast, the latter hypothesis predicts that the frequency of large sectors would be roughly equivalent to the square root of the frequency of sectors half their size. In 655 pinnae sampled, sectors over 50% of the pinna length occurred 88 times, sectors occupying 25-50% occurred 122 times and sectors occupying 12.5–49.9% occurred 207 times. Large sectors are thus derived from a single cell because the frequency is roughly half that of smaller sectors.

Modelling

We assumed that the probability, p, of a cell turning green to yellow was fixed for all divisions within the life cycle. Where a single cell gives rise to a subset of cells, e.g. a single initial forms a number of pinnae by successive divisions, the probability of each pinna being yellow is given by a different conditional probability. For example, if one green cell gives rise to three cells, each of which is the founding cell of a pinna then the conditional probability of the first pinna being entirely yellow is p, of the second is $p(1+q)$ and of the third is $p(1+q+q^2)$, where $q=(1–p)$. The average probability of a random chosen pinna being yellow is thus $p(3+2q+q^2)/3$ – this corresponds to the observed frequency of yellow pinnae (P_{obs}).

To model fern sector patterns, we needed an estimate of the unknown unconditional mutation probability, p. To get this estimate, P_{obs} was first calculated for the sample population. The unconditional probability was then calculated using P_{obs} together with the hypothesized patterns of cell divisions. For example, given the three cell division rounds above, $P_{obs}=(p + pq + pq^2)/3$ and the unconditional probability is obtained by solving the equation for p.

Each model of the development of contiguous yellow pinnae distributions had two design parameters. The first described the number of pinnae developing from each merophyte initial (Np), while the second described the cell division sequence of the initial. These divisions were classified as birfurcations or as sequential divisions with asymmetric cell fates. For each division a random number from 0-1 was assigned to the dividing cell and if that number had the same value or less than p then the cell was assumed to turn yellow. The model was used to generate one million pinnae as a continuous linear sequence that was then scanned to estimate the number of 1, 2, 3, 4 or 5 contiguous yellow pinnae. Ninety-five percent prediction intervals of the proportion of contiguous pinnae in each integer category were then generated by repeated sub-sampling of 7160 pinnae sequences from this simulated dataset. All simulations were conducted in MATLAB.

Models of sectors within individual pinnae were developed using a similar approach to that above. Both bifurcation and sequential, asymmetric cell-fate division models were investigated for the first few divisions that would generate five large yellow sectors in different positions of the pinna if a transition occurred.

RESULTS

Sectors in variegated *Nephrolepis exaltata* are cell-autonomous

N. exaltata cv. *bostonensis* plants are highly variegated (Fig. 1A,B) with yellow sector sizes ranging from one cell within the lamina of a pinna to a number of contiguous fronds. Yellow sectors are formed spontaneously through an unknown genetic or epigenetic mechanism. Importantly, sectors have regular and predictable shapes, indicating that they are clonal in origin. Measurement of the number of small (i.e. not touching the margin or midrib) yellow sectors within green pinna tissue and of small green sectors within yellow pinna tissue show that reversion events can occur, but that they are 80 times less likely than forward events. At the subcellular level, sectors can be defined by differences in chlorophyll autofluorescence, with green sectors fluorescing more brightly than yellow sectors (Fig. 1C,D). Single yellow cells can be surrounded by green cells (Fig. 1E), indicating that the conversion mechanism operates at the single cell level (i.e. is cell-autonomous). This cell autonomy validates the use of the line for lineage analysis.

Leafy shoots are generated from a single persistent apical initial

N. exaltata produces rhizomatous shoots that initiate erect leafy shoots (Fig. 2A). Transverse sections show that fronds arise in a helical phyllotaxy from leafy shoots (Fig. 2B-E) and in longitudinal section, a presumptive single initial cell can be seen at the apex (Fig. 2F). To confirm the actual number of apical initials producing

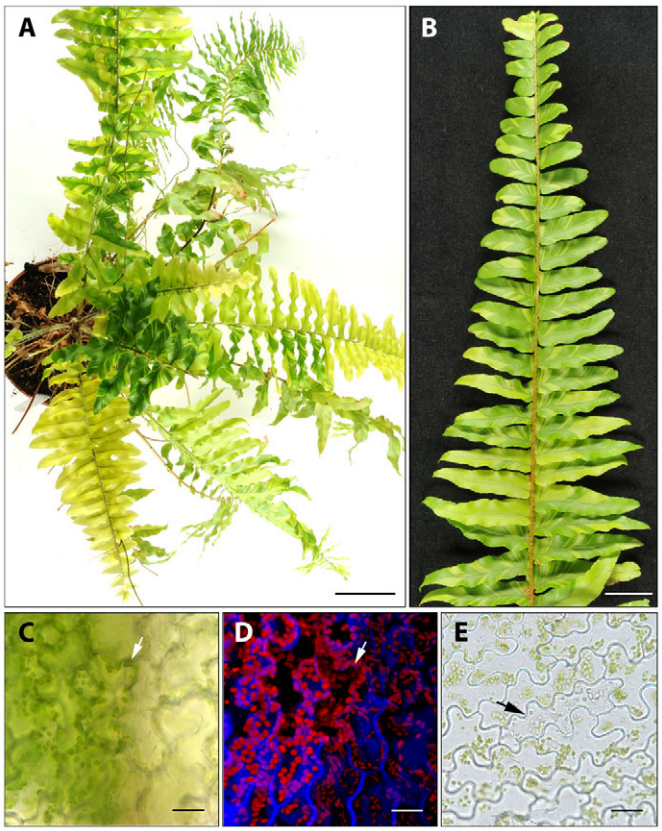

Fig. 1. Sectors are cell-autonomous. (**A**) *Nephrolepis exaltata* cv. *bostonensis* whole plant. Scale bar: 30 mm. (**B**) *N. exaltata* frond. Scale bar: 20 mm. (**C**) Paradermal view of sector boundary. Arrow indicates equivalent position in D. Scale bar: 50 μm. (**D**) Confocal image of sector boundary in C. Chlorophyll autofluorescence, red; calcoflour stained cell walls, false coloured blue; arrow indicates equivalent position in C. Scale bar: 50 μm. (**E**) Paradermal view of single cell sector in epidermal peel. Arrow indicates wall between cells with green and pale chloroplasts. Scale bar: 70 μm.

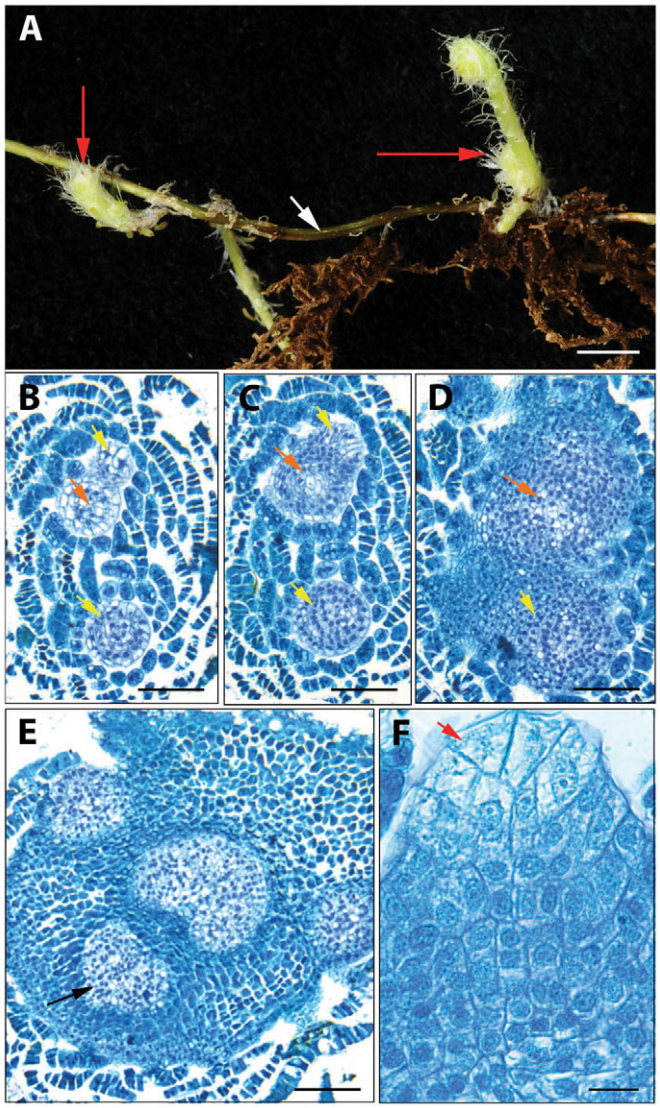

Fig. 2. The leafy shoot produces fronds in a helical phyllotaxy. (**A**) Leafy shoots (red arrows) on a rhizome (white arrow). Scale bar: 10 mm. (**B-E**) Distal (B) to proximal (E) cross-sections (10 μm thickness) at 20-50 μm intervals through a leafy shoot. Orange arrows, shoot apex; yellow arrows, early fronds; black arrow, frond vascular trace. Scale bars: 500 μm. (**F**) Longitudinal section showing presumptive apical initial (red arrow). Scale bar: 10 μm.

the leafy shoot, sequences of yellow fronds arising from different shoots were recorded. If multiple apical cells form the shoot, sectors would span successive fronds in a segment of the shoot diameter and the segment size would be inversely proportional to the apical cell number (Table 1, upper panels). By contrast, if the shoot were produced from one cell, yellow sectors would span all successive fronds around the shoot and would continue to the apex (Table 1, lower panels). Table 1 shows that of the 67 shoots examined (each comprising at least five fronds), no multi-frond sectors occupying a segment of the shoot were identified, whereas seven sectors spanned successive fronds and continued to the apex. The remaining 60 shoots did not have contiguous sequences of yellow fronds and were thus not informative. These frequencies strongly suggest that the leafy shoot is derived from a single apical initial.

Individual fronds arise from a single initial

To determine how the leafy shoot initial generates fronds, the position and frequency of all yellow fronds was documented. If a derivative of the shoot apical initial generates multiple fronds, sectors encompassing multiple fronds positioned between variegated fronds would be common. Alternatively, if derivatives of the apical initial generate a single frond, multi-frond sectors would be rare and single yellow fronds would be common. Of the 67 shoots sampled, 28 sectors occupied a single frond and two sectors occupied two fronds (Fig. 3A; Table 2). No sectors occupied three or more successive fronds unless they continued to the apex (as in Table 1). These frequencies suggest that each frond develops from a single cell and that sectors occupying two fronds results from two independent events.

Frond initial cells are persistent and apical

To characterize how fronds are formed from a single cell, the size and distribution pattern of yellow sectors that encompassed multiple pinnae within a frond were recorded for 114 randomly sampled fronds. Sectors occurring on one side of the rachis were

Table 1. Analysis of shoot apical initials

Hypothesis	Prediction	Number observed
Three initials	Sector traversing one-third of shoot	0
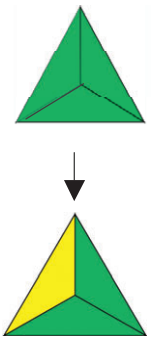	Top-down view 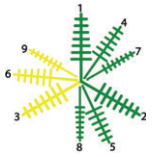 Side-on view 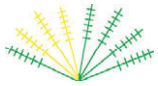	
One initial	Sector across successive fronds	7
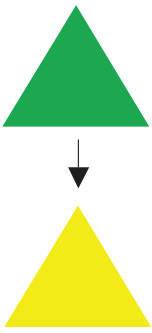	Top-down view 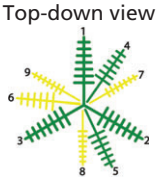 Side-on view 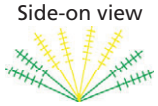	
	Plants showing neither pattern	60

Hypothesized number and phenotype of cells at the shoot apex (triangle) following a green to yellow transition, with consequent patterns of sectors in fronds 1-9, where 1 is the oldest and 9 is the youngest.

encountered throughout the frond and always comprised five or fewer contiguous pinnae (see Table S1 in the supplementary material). By contrast, sectors of more than five contiguous pinnae always spanned both sides of the rachis, occurred at the distal tip (e.g. Fig. 3B) and occupied 6-100% of the frond length (Fig. 3C). The lack of large rachis-spanning sectors at the frond base or middle demonstrates that the initial is located at the tip of the frond. If the apical initial was transient, sectors occupying 100% of the frond length would be the result of at least two independent mutations and would thus be less common than distal sectors occupying smaller percentages of the length. However, sectors that occupy 100% of the frond length occurred more frequently than distal sectors of any other size. Therefore, a single persistent apical initial must give rise to the entire frond.

The frond apical initial produces merophyte initials that contribute to half of the mediolateral axis

Confocal microscopy reveals a single wedge-shaped cell at the frond apex presumed to be the apical initial. The presumptive initial (Fig. 4, red) has two external cutting faces that extend across the ad-abaxial plane. The orientation of the cutting faces suggests that the initial divides obliquely and alternately to successively produce merophyte initials in the mediolateral plane (Fig. 4A-C,E,G, grey). The cell wall patterns further suggest that each merophyte initial then divides periclinally to produce medial cells in the rachis (Fig. 4B,G, orange) and lateral cells on the flanks (Fig. 4B,G, purple). The medial cells are located directly below the frond initial (Fig. 4H, orange) but are probably not derived directly from it. If these inferences are correct, periclinal divisions of the medial derivatives of the merophyte increase cell number in the mediolateral axis, and anticlinal divisions of the medial and lateral derivatives increase cell number in the proximodistal axis. Histological analysis therefore suggests that a mutation in a merophyte initial would produce a sector occupying half of the mediolateral axis and a limited section of the proximodistal axis.

To test whether division patterns at the apex of the frond are as inferred above (Fig. 4I), sector patterns were observed within 60 young fronds where colour variation on the rachis was visible. Thirty-eight sectors encompassing the right side of the mediolateral axis and 49 sectors encompassing the left side were observed (Figs 4J,K). Such sectors most commonly spanned one to five pinnae in the proximodistal axis (Fig. 4L-N) and between one-third and two-thirds of the rachis in the mediolateral axis (Fig. 4O-Q). Rachis sectors extended to varying degrees in the proximodistal axis, terminating either adjacent to pinnae or midway between pinnae. Sectors encompassing a pinna and a region of rachis indicate that pinnae and adjacent rachis can be derived from a single cell (Fig. 4P), confirming inferences from histological images (Fig. 4A-C). However, because sectors occur that encompass a segment of rachis between two pinnae (Fig. 4R), parts of the rachis can be derived from cells lying between those that give rise to pinnae. Such rachis-only sectors were rarely observed, possibly owing to their small size. In combination, these sector patterns confirm that each merophyte initial contributes pinnae and rachis to half of the mediolateral frond axis.

Fig. 3. Fronds arise from a single apical initial. (**A**) Entirely pale frond (red arrow) flanked by variegated fronds (white arrows). Scale bar: 10 mm. (**B**) Frond with entirely pale distal third. Scale bar: 20 mm. (**C**) Data from 14 fronds showing variation in the proportion of the frond exhibiting a distal pale sector.

Merophyte initials contribute units of three pinnae to the proximodistal frond axis

To determine more precisely the relative contribution of a single merophyte initial to the proximodistal frond axis, we first examined the frequency and distribution of contiguous sequences of entirely yellow pinnae in 114 randomly sampled fronds (a total of 7160 pinnae) (see Table S1 in the supplementary material). Two sectors spanned five pinnae, three spanned four, 25 spanned three, 37 spanned two and 124 spanned a single pinna. The conditional probability (P_{obs}) of the green to yellow transition (i.e. the probability that a randomly selected pinna is yellow) was thus calculated as 0.041 on the basis that 295 out of the 7160 observed pinnae were yellow. P_{obs} was then used to calculate the unconditional probability (i.e. the probability of a given cell mutating to yellow) for six putative patterns of cell division (Fig. 5; see Table S2 in the supplementary material). These division patterns were classified as bifurcations (Fig. 5A) or as sequential divisions with asymmetric cell fates (Fig. 5B-F). Models were generated that simulated each of the division patterns, with the number of pinnae (Np) ultimately produced varying from two to five (see Table S2 in the supplementary material). Only values of Np that gave the best fit to each model are shown in Fig. 5. In the first model, the lateral derivative (Fig. 5, purple) undergoes successive bifurcations to produce cells that each generate pinnae and part of the rachis (Fig. 5A, Np=4). In an alternative model, pinna progenitor cells are specified in a staggered manner, such that divisions of the lateral derivative either generate one daughter cell that gives rise to a pinna and another daughter that divides again to produce two pinna progenitor cells (Fig. 5B, Np=3), or at each division one daughter cell gives rise to a pinna and these divisions are repeated (Fig. 5C, Np=3). In these latter two scenarios, regions of rachis could either be derived as a late division from the same cell as the pinna (Fig. 5B,C) or from distinct derivatives of the division process (Fig. 5D,E, Np=3).

To determine which of the proposed models is more likely, a computer model generated predictions of the expected frequency of different sector sizes given each cell division pattern and Np (Fig. 5A-E; see Table S2 in the supplementary material). Analysis of the model simulations showed no support for any model of cell division with fewer or more than three pinnae per lateral derivative of a merophyte initial. The best-fit with 3<Np<3 was provided by a bifurcation model (Fig. 5A) but it is clear that this model does not fit the pattern of sectors observed (i.e. the model failed to generate enough sectors spanning three pinnae and generated too many that spanned four). For the sequential asymmetric division model with 3<Np<3, the distribution of sectors was also very different from that observed. There was thus overwhelming evidence that Np=3 (see Table S2 in the supplementary material). Because sectors occur spontaneously, two independent mutation events could occur in adjacent merophyte initials resulting in sectors that span more than three pinnae, but such sectors would occur at a much lower

Table 2. Analysis of frond initial cells

Hypothesis	Prediction	Number observed
Sequential fronds arise from a shared cell population	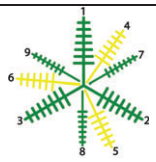 Sectors spanning numerous fronds but flanked by variegated fronds	2
Individual fronds arise from distinct cell populations	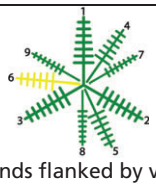 Single yellow fronds flanked by variegated fronds	28

Pattern of sectors in fronds 1-9, where 1 is the oldest and 9 is the youngest.

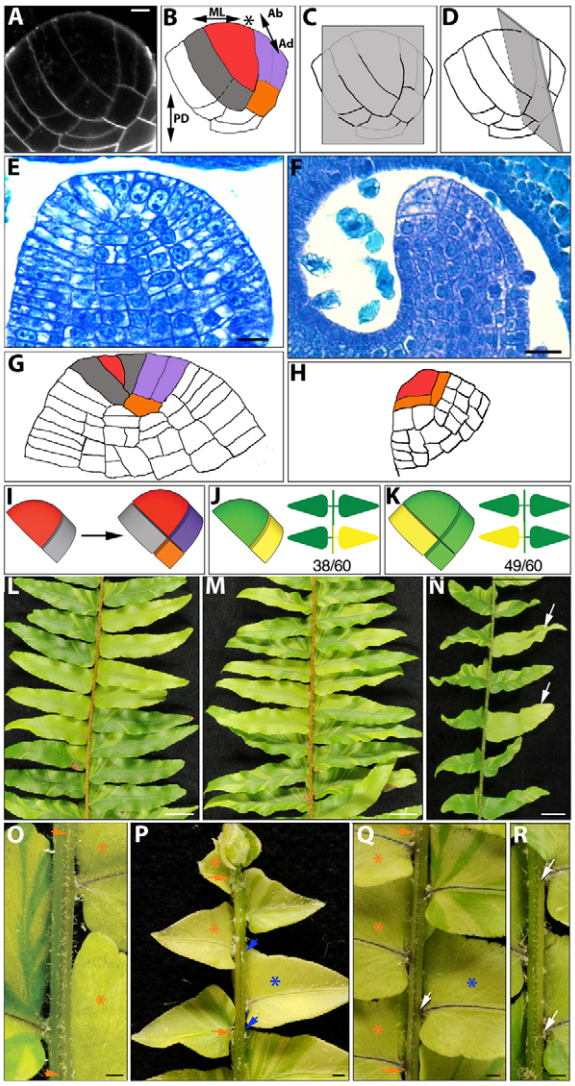

Fig. 4. Frond apical initials produce merophyte initials that contribute to half of the mediolateral axis. (**A**) Confocal image of frond apex stained with calcofluor white to highlight cell walls. Scale bar: 5 μm. (**B**) Line drawing of apex in A showing presumptive apical initial cell (red), merophyte initial (grey), lateral (purple) and medial (orange) products of the merophyte initial. Asterisk indicates the position of next merophyte initial; dotted line indicates that new cell wall is forming; arrows indicate proximodistal (PD), mediolateral (ML) and ad-abaxial (Ad, Ab) axes. (**C**) Schematic of apex in A. Grey box indicates the plane of section in E. (**D**) Schematic of apex in A. Grey box indicates the plane of section in F. (**E**) Longitudinal section of frond apex (as in C). Scale bar: 20 μm. (**F**) Sagittal section of frond apex (as in D). Scale bar: 30 μm. (**G**) Line drawing of section in E. Presumptive apical initial, red; merophyte initials, grey; first products of merophyte initials, purple and orange. The purple derivative has undergone a further division when compared with B. (**H**) Line drawing of apex in F. Presumptive apical initial, red. Cells below the apical initial (orange) probably arise from divisions of the merophyte initials (not visible). (**I**) Schematic of inferred first two rounds of division. The apical initial cell (red) produces a merophyte initial (grey) and then gives rise to a second merophyte initial (grey), while the first divides periclinally to produce a medial (orange) and lateral (purple) cell. (**J**,**K**) Schematic of frond apex with predicted sector pattern and frequency of sectors observed on 60 fronds. Mutations in the merophyte initials, result in sectors that encompass pinnae on the right (J) or left (K) side of the frond. (**L**,**M**) Sectors encompassing numerous pinnae. Scale bars: 10 mm. (**N**) Single pinna sectors (arrows). Scale bar: 10 mm. (**O**) Sector encompassing two pinnae (orange asterisks) and one-third to one-half of the rachis in the mediolateral axis (between orange arrows in the mediolateral axis). Scale bar: 2 mm. (**P**) A sector encompasses at least two pinnae (orange asterisks) and one-third to one-half of the rachis, and continues into the crosier (orange arrows). Another sector encompasses a single pinna (blue asterisk) and a small region of rachis in the proximodistal axis (between the blue arrows). Scale bar: 2 mm. (**Q**) A sector encompasses three pinnae (orange asterisks) and adjacent rachis (orange arrows). Another sector encompasses a single pinna (blue asterisk) but does not extend into the rachis (at the white arrow). Scale bar: 2 mm. (**R**) Sector (between white arrows) encompassing one-third to one-half of the rachis in the mediolateral axis between two variegated pinnae. Scale bar: 2 mm.

frequency than sectors spanning one, two or three pinnae. Sequences of six yellow pinnae would be extremely rare, as they would require both adjoining cells to mutate at the first divisional stage. Multiples of three are thus predicted to be rarer than multiples of three minus one or minus two. Notably, the graphs in Fig. 5B,C,E fit more closely the data than the model of successive bifurcations in Fig. 5A, and thus the three-pinna units result from a process of sequential asymmetric cell divisions.

To understand the relative contribution of cells to pinnae versus portions of the rachis in the three-pinna units, further models were tested predicting sector sizes with later cell divisions (see Table S2 in the supplementary material). The best supported model simulated later cell divisions, giving rise to cells that either produce both a pinna and part of the rachis, or produce just part of the rachis (Fig. 5F). This model agrees with observed morphology and sector patterns. For example, mutations in cells that produce both pinna and rachis will give sectors as in Fig. 4P (blue asterisks and arrows) and those in cells that produce just rachis will give sectors as in Fig. 4R. Predictive modelling and observed sector frequencies thus suggest that single merophyte initials first divide asymmetrically to produce a medial and lateral derivative. The lateral derivative then divides in a staggered anticlinal manner to produce a unit comprising three pinnae and associated rachis along the proximodistal axis. The sequential production of merophyte initials from the apical initial thus leads to iterative development of the frond.

Pinna development is initiated by a single cell on the flanks of the frond

Sectors encompassing a single pinna and part of the rachis (Fig. 4P) demonstrate that individual daughter cells of the lateral derivative of the merophyte initial contribute both pinnae and rachis to the mediolateral frond axis. However, because single pinnae can be exclusively yellow (Fig. 4Q), and are found at a relatively high frequency (at least 4.1%), individual pinnae presumably subsequently arise from a single cell. To examine pinna development, immature fronds were first viewed by SEM (Fig. 6A,B). Pinnae emerge from the flanks of the frond just a few cells below the apex (Fig. 6B, arrowhead) in a region that comprises files of elongated epidermal cells and a central core of smaller cells (Fig. 6C,D). As pinnae are initiated, three to five of these epidermal cells bulge out from the frond rachis (Fig. 6E,F,

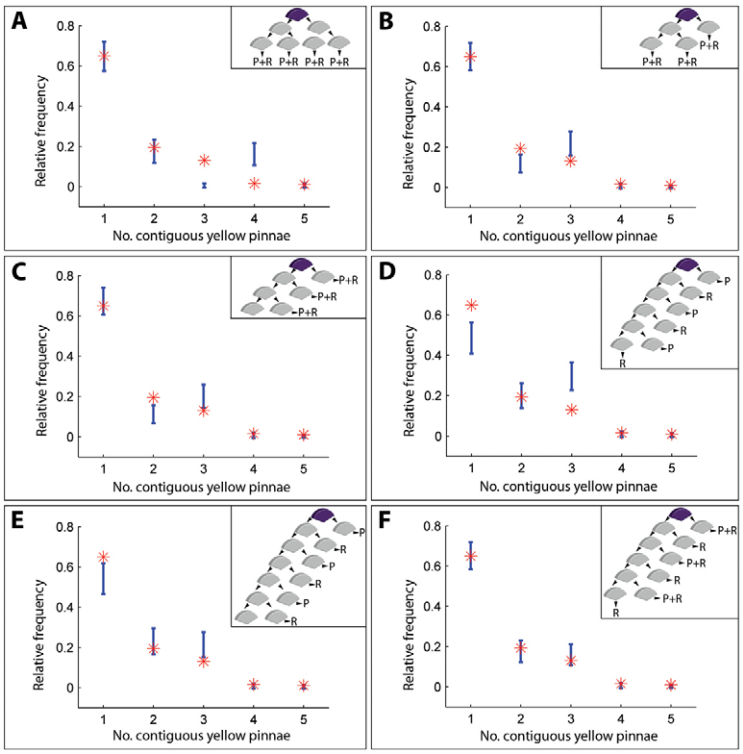

Fig. 5. Merophyte initials contribute units of three pinnae to the proximodistal frond axis. Simulated 95% prediction intervals of the frequency of 1-5 contiguous yellow pinnae (blue) generated by possible cell division patterns of the lateral derivative of the merophyte initial (purple) shown in each inset box, with observed frequencies shown in red. The purple derivative has either cleaved directly from the merophyte initial (indicated by 1) or has undergone an additional round of division as in Fig. 4G (indicated by 2). P, pinnae; R, rachis segments. (**A**) The cell bifurcates producing two cells that each bifurcate again to generate cells that form pinna and rachis components. (**B**) An iterative model where the cell divides to produce one daughter that forms pinna and rachis components and a second daughter that continues dividing, eventually bifurcating to produce two daughters that each form pinna and rachis components. (**C**) As in B, except the final division remains asymmetric rather than a bifurcation. (**D**) As in B, except that the first daughter cell from each division forms pinna or rachis in alternating sequence. (**E**) As in D, except the final division remains asymmetric rather than a bifurcation. (**F**) As in D, except the first daughter from each division forms pinna and rachis, or rachis only, in alternating sequence.

black arrowheads), contributing cells to the mediolateral pinna axis and the proximodistal frond axis. Periclinal divisions then occur on the two internal faces of these cells (Fig. 6F, green arrowheads) contributing derivatives to the proximodistal and ad-abaxial pinna axes.

Apical and marginal initials co-ordinately generate the determinate pinna

To assess patterns of cell division in the pinna, within-pinna sectors were examined. Most sectors occupying less than one-fifth of a pinna length are roughly rhomboid, with the long axis extending from midvein to margin (Fig. 7A, red arrow). Some sectors broaden marginally such that the sector occupies a greater proportion of the lamina at the margin than at the midvein (Fig. 7A, black arrow). Late sectors in the lamina are much smaller but are orientated in the same manner (Fig. 7B, arrows). The shape and size of late sectors indicates that divisions extending the proximodistal pinna axis cease before those that expand the mediolateral axis.

To understand how the proximodistal pinna axis is elaborated, sector patterns on 655 randomly sampled pinnae were analysed in terms of length along the midvein. One-hundred and thirty-eight of the sampled pinnae were all yellow, giving an average conditional probability (P_{obs}) of the green to yellow transition of 0.061. Early cell division patterns of the pinna initial were deduced on the basis that sectors of approximately one-third midvein length were observed on one or other side of the midvein in the base or middle of the lamina but on both sides of the midvein at the tip of the lamina. Fig. 7C quantifies the data for 125 variegated pinnae by showing the relative positions of such sectors along the midvein. These data support a model whereby the apical initial normally undergoes two rounds of anticlinal cell division, cleaving derivatives to both left and right sides in each round, with each derivative making a substantial contribution to the pinna (Fig. 7D-H). The unconditional frequency (p) of the green to yellow transition for the model shown in Fig. 7D-H was 0.0117. Pinnae are asymmetric in that a lobe is produced on one side at the base. The relative frequencies of 'handed' sectors that are positioned asymmetrically across the midvein (as in Fig. 7E,G) suggest that in the first round of division, the first daughter cell is most often (25/31) cleaved to the lobe side. By contrast, in the second round of division the first daughter cell is equally likely to be cleaved to the lobe (18/33) (as in Fig. 7G) or non-lobe (15/33) side. This pattern of cell division is confirmed through the close agreement of predicted and observed sector frequencies (Fig. 7I).

To assess further the relative contribution of the pinna apical cell and its derivatives, sectors were examined in the midvein and in the ad-abaxial pinna axis. Chloroplasts surrounding the midvein were always phenotypically identical to those in the most distal third of the lamina (Fig. 7J,K). Given that the lamina and midvein at the base of the pinna can be phenotypically different (Fig. 7J,K), the apical initial and its derivatives must contribute varying amounts to the mediolateral and proximodistal pinna axes. In support of this suggestion, SEMs of developing pinnae show that the apical initial divides longitudinally to contribute cells to the mediolateral lamina axis and transversely to extend the midvein in the proximodistal axis. By contrast, the derivatives divide longitudinally to extend the proximodistal lamina axis and obliquely to expand the mediolateral lamina axis (Fig. 7L). As a consequence, the central region of the pinna is primarily generated by the apical initial (Fig. 7M, pink), while the marginal regions are generated by the derivatives acting as marginal initials (Fig. 7M, white). Although morphological studies suggest that cell divisions always cease last at the apex (data not shown), the variable contribution of marginal initials influences final pinna morphology. Notably, all sectors that touch the margin encompass all cell layers in the ad-abaxial axis (Fig. 7N), whereas sectors that do not touch the margin do not span all layers (Fig. 7O). This observation

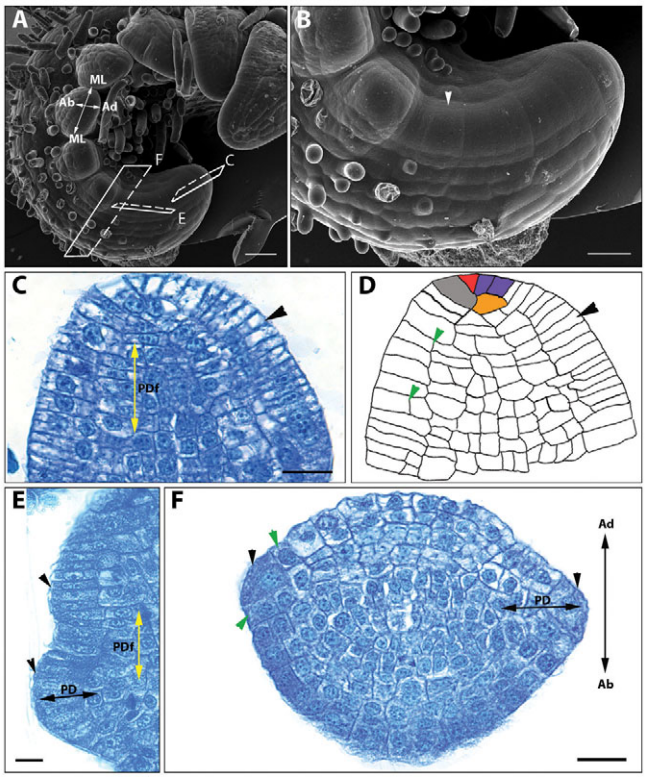

Fig. 6. Pinnae initials arise from the frond flanks. (**A**) SEM of frond apex showing pinnae initiating. Boxes indicate section planes in C,E and F. Mediolateral (ML) and ad-abaxial (Ad, Ab) axes are indicated. Scale bar: 20 μm. (**B**) Higher magnification of frond apex. A slight bulge (white arrowhead) marks an emerging pinna. Scale bar: 15 μm. (**C**) Longitudinal section of frond apex showing elongated epidermal cell files on the flanks (arrowhead). Yellow double-headed arrow indicates proximodistal axis of the frond (PDf). Scale bar: 20 μm. (**D**) Line drawing of section in C. Black arrowhead, epidermal cell files on the flank; green arrowheads, medial divisions of epidermal cells. (**E**) Longitudinal section of frond apex showing emerging pinnae (arrowheads). Black double-headed arrow, proximodistal pinna axis (PD); yellow double-headed arrow, PDf. Scale bar: 10 μm. (**F**) Transverse section of developing frond showing pinnae (black arrowheads) emerging on both sides of rachis. Internal cell divisions from two cutting faces are evident (green arrowheads). Double-headed arrows indicate PD and ad-abaxial (Ad,Ab) pinna axes. Scale bar: 20 μm.

suggests that the lamina is derived predominantly from a single layer of cells at the pinna margin, and demonstrates that the ad-abaxial axis is established after the proximodistal and mediolateral axes.

DISCUSSION

A novel approach that combines sector analysis, histology and predictive conditional probability modelling methods has been used to elucidate how shoot form is elaborated in the fern *N. exaltata*. The data presented show that shoots, fronds and pinnae all develop from single apical initial cells (Tables 1, 2; Figs 2, 3, 6), that both shoots and fronds develop iteratively (Figs 2, 4, 5), and that pinnae develop from marginal meristems (Fig. 7). The use of software simulations to test hypotheses of cell division patterns has provided insight into frond development at a much finer resolution than has been previously achieved and has demonstrated that the specification of pinna plus rachis fate, as opposed to rachis only, occurs in adjacent cells.

The robustness of the predictive models is dependent on an accurate estimation of the unconditional probability of the green to yellow transition (p). We estimated p in two different parts of the fern (within-fronds and within-pinnae) using methods and cell-division models that were sufficiently different that they are effectively independent estimates. We estimated p within-fronds as 0.007 and within-pinnae as 0.0117. We also observed that green to yellow transitions were 80 times more frequent than yellow to green reversions in pinnae. Assuming the simplest model, where the reversion frequency is the squared probability of the transition frequency, this would yield an estimate of 0.0125 for p. We are thus confident that the probability estimates are reliable. Given that any of these values could range independently from 0 to 1, the close agreement of all three provides strong support for the predictive cell-division models in Fig. 5 (fronds) and Fig. 7 (pinnae).

Developmental mechanisms in *N. exaltata* are likely to be representative of most ferns

Although it is always difficult to assess the degree to which data from a single species can be used for wider inference, morphological studies of early fern development have shown many commonalities. For example, surface examination of the shoot apex of numerous species reveals a tetrahedral apical cell with three cutting faces (Bierhorst, 1977) similar to that seen in *N. exaltata* (Fig. 2). Likewise, developing frond primordia shown in other studies (Bierhorst, 1977; Richards et al., 1983; White and Turner, 1995) closely resemble those of *N. exaltata* (Fig. 4). Furthermore, despite the morphological diversity of leptosporangiate ferns, many comprise fronds with a rachis and lateral pinnae, and all develop from crosiers (Gifford and Foster, 1989). Notably, even where differences in apical initial number have been reported, patterns of organ development are conserved. For example, pinnae of *Ceratopteris richardii* sporophylls develop from two apical initials, but, as in *N. exaltata*, the initials divide anticlinally to generate marginal initials that contribute to most of the lamina, and periclinally to contribute the central core and midvein of the pinna (Hill, 2001). In combination, these observations suggest that the mechanisms elucidated in *N. exaltata* provide a framework for understanding the development of other polypod ferns, the group that contains over 80% of all living fern species (Pryer et al., 2004).

Fern fronds are developmentally equivalent to shoots

Both shoots and fronds of the fern *N. exaltata* exhibit iterative growth patterns, whereby sequential derivatives of apical initials give rise to repeating segments of the final structure. The shoot apical initial iterates fronds, and the frond apical initial iterates units of three pinnae in the proximodistal axis that contribute to half of the mediolateral frond axis. The potential for frond primordia to develop into shoots has previously been demonstrated in vitro and has been interpreted to mean that determinacy is delayed in fern fronds when compared with seed plant leaves (e.g. Cutter, 1956) (for a review, see White and Turner, 1995). However, our data demonstrate that fronds inherently develop in an iterative manner. Interestingly, morphologists have previously suggested that fronds, as the dominant vegetative structure in ferns, are subject to the same selective pressures as shoots in other land plant groups (Kaplan, 1996). This suggestion is notable in the context of our findings because iterative growth processes permit flexibility in the face of environmental challenges.

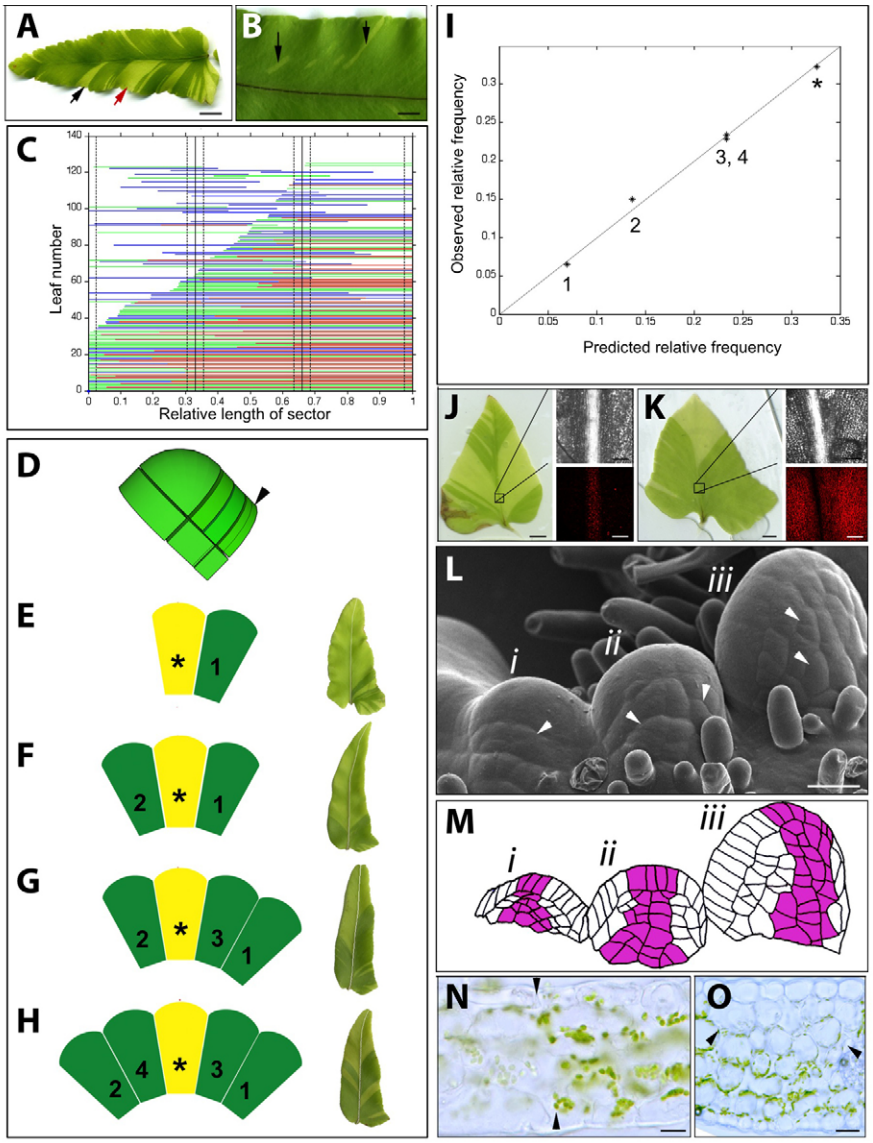

Fig. 7. Pinna initials gives rise to marginal derivatives that, together with the initial, generate the lamina. (**A**) Pinna with lamina sectors. Sectors are often roughly rhomboid (red arrow) or broaden marginally (black arrow), with the long axis running midrib to margin. Scale bar: 10 mm. (**B**) Small sectors that terminate between the margin and midrib. Scale bar: 3 mm. (**C**) Graph showing relative length and position of sectors occupying over 33% of the pinna length. Base of pinna is at 0 and tip at 1. Blue lines indicate sectors on left side of midvein; green lines indicate the right side; red lines indicate sectors present both sides. Vertical broken lines indicate the ±2.5% error margins on sector boundaries. (**D-H**) Schematic of cell division sequence of pinna progenitor cell and examples of resultant sectors, shown as actual pinnae observed. The initial cell is indicated by a black arrowhead in relation to frond initial (D) and by asterisks in longitudinal section (E-H). Initial cell derivatives are numbered in the order they are generated (E-H). Early cell divisions are anticlinal, producing a cell on either side of the initial cell (E,F). A mutation in the initial cell after the first division produces a sector encompassing the entire lamina on one side and the entire apical region (E). A sector in the initial cell following the first two divisions produces a sector spanning the mid-vein and apical region of the pinna (F). Further anticlinal divisions of the initial cell facilitate a bulge on the rachis flanks (G,H; as in Fig. 6B). The third derivative is equally likely to be cleaved to the left or right. Only the right-hand version is shown here. A mutation in the initial cell following the third division produces a sector encompassing the apical region on both sides and extending basally along the rachis on one side of the mid-vein (G). A mutation in the initial cell following four divisions produces a sector spanning the pinna tip that is smaller than that in F (H). (**I**) Graph showing observed and predicted (from a conditional probability model of cell division) frequencies of yellow sectors generated in cell positions 1, 2, 3, 4 and * in D-H. (**J**) Pinna with large regions of yellow lamina but green tip and midvein. Scale bar: 2 mm. Bright-field and confocal images are shown in the boxes. Scale bars: 500 μm. (**K**) Pinna with green lamina at the base but yellow at the tip and midvein. Scale bar: 2 mm. Bright-field and confocal images are shown in the boxes. Scale bars: 500 μm. (**L**) SEM of developing pinnae. Examples of oblique cell divisions are indicated with white arrowheads. Roman numerals correspond to schematics in M. Scale bar: 50 μm. (**M**) Schematic of pinnae in L with cells likely to be derived from the apical initial in pink and cells likely to be derived from the four flanking cells in white. (**N**) Fresh cross-section of pinna lamina with a sector touching the pinna margin that traverses the entire ad-abaxial axis. Sector boundaries are indicated by black arrowheads. Scale bar: 30 μm. (**O**) Fresh cross-section of pinna lamina with a sector not touching the margin. The sector encompasses two out of the five internal cell layers in the ad-abaxial axis. Sector boundaries are indicated by black arrowheads. Scale bar: 30 μm.

Although the process underpinning frond development is shoot-like, morphologically fronds have leaf-like properties such as dorsiventral flattening and bilateral symmetry. In considering these properties and the extent to which fronds are equivalent to leaves, the most obvious comparison to make is with compound leaves of seed plants. As in compound leaves, development in *N. exaltata* fronds is not strictly indeterminate because growth eventually ceases after the formation of around 80 pinnae. However, true indeterminacy is not always a feature of shoots in that some seed plant shoots terminate in flowers, and some fronds (Clarke, 1936) and compound seed plant leaves (Steingraeber and Fisher, 1986) are indeterminate. Mechanisms underpinning compound leaf formation have been studied in three main model organisms (tomato, pea, *Cardamine hirsuta*) and in each case it has been demonstrated that leaf morphology is elaborated through the spatial and/or temporal induction of localized cell divisions within developing primordia (for reviews, see Bharathan and Sinha, 2001; Tsiantis and Hay, 2003). In *C. hirsuta*, lineage analysis has further demonstrated that lateral leaflets are initiated from cells at the margin of the rachis by an auxin-associated pathway similar to that used for leaf initiation at the shoot apical meristem (Barkoulas et al., 2008). However, lateral leaflets are formed after the terminal leaflet and rachis have differentiated, and there is no evidence of iterative apical growth. These observations suggest that shoot and compound leaf development programs are fundamentally different and that any similarities between genetic pathways operating in the

C. hirsuta shoot and leaf reflect the co-option of 'shoot' pathways into the compound leaf developmental program. Fern fronds are thus more similar to dorsiventrally flattened shoots than to compound leaves.

Pinnae are determinate organs that develop from apical and marginal initials

N. exaltata pinnae are determinate organs on the lateral flanks of the rachis. Unlike fronds, pinnae exhibit a growth pattern whereby the single apical initial first gives rise to a few derivatives that act as marginal initials. The apical and marginal initials are then coordinately regulated to generate the final pinna morphology. The apical initial generates the most distal third of the lamina plus the central core, including the midvein, while each marginal initial normally generates the basal- or mid-third of the lamina on one side of the midvein. The coordinated activity of a subset of cells during pinna development is equivalent to that seen in leaf-like organs of bryophyte gametophytes, microphylls of lycophytes and simple leaves of seed plants.

Evolution of land plant shoots

The Telome theory suggested that leaves of both ferns and seed plants evolved from branches (Zimmermann, 1952). The finding that fern fronds have inherent shoot-like properties is consistent with this suggestion. If we assume that the bifurcating stems of extant lycophytes and ferns are similar to the dichotomizing leafless axes of early land plants, then the dichotomy was established following the division of a single shoot apical initial into two identical daughter initials (Bierhorst, 1977; Harrison et al., 2007; Jones and Drinnan, 2009). This scenario allows for evolutionary progression to the formation of fronds if instead of dividing equally, the shoot apical initial divides to renew the shoot apical initial and to generate a daughter with modified developmental potential (the frond apical initial). The question still remains, however, of how those modified shoots (fronds) evolved to produce leaves (pinnae).

Acknowledgements

We thank Jill Harrison and Liam Dolan for discussions about sector analysis; Hugh Dickinson, Paula Rudall, Richard Bateman and Kevin Boyce for discussions about morphology; Ian Moore for assistance with confocal; and Julie Bull and John Baker for technical support. This work was supported by grants from The Gatsby Charitable Foundation and the ERC to J.A.L.

Competing interests statement

The authors declare no competing financial interests.

Supplementary material

Supplementary material for this article is available at
http://dev.biologists.org/lookup/suppl/doi:10.1242/dev.065888/-/DC1

References

Barkoulas, M., Hay, A., Kougioumoutzi, E. and Tsiantis, M. (2008). A developmental framework for dissected leaf formation in the Arabidopsis relative *Cardamine hirsuta*. *Nat. Genet.* **40**, 1136-1141.
Berlyn, G. P. and Miksche, J. P. (1976). *Botanical Microtechnique and Cytochemistry*. Ames, IA: Iowa State University Press.
Bharathan, G. and Sinha, N. R. (2001). The regulation of compound leaf development. *Plant Physiol.* **127**, 1533-1538.
Bierhorst, D. W. (1977). On the stem apex, leaf initiation and early leaf ontogeny in filicalean ferns. *Am. J. Bot.* **64**, 125-152.
Bower, F. O. (1884). On the comparative morphology of the leaf in the vascular cryptogams and gymnosperms. *Philos. Trans. R. Soc. Lond. B* **175**, 565-615.
Bower, F. O. (1935). *Primitive Land Plants*. London: Macmillan.
Clarke, H. M. (1936). The morphology and anatomy of *Lygodium japonicum*. *Am. J. Bot.* **23**, 405-413.
Crane, P. R. and Kenrick, P. (1997). Diverted development of reproductive organs: a source of morphological innovation in land plants. *Plant Syst. Evol.* **206**, 161-174.
Cutter, E. G. (1956). Experimental and analytical studies of pteridophytes. XXXIII. The experimental induction of buds from leaf primordia in *Dryopteris aristata* Druce. *Ann. Bot.* **20**, 143-165.
Floyd, S. K. and Bowman, J. L. (2006). Distinct developmental mechanisms reflect the independent origins of leaves in vascular plants. *Curr. Biol.* **16**, 1911-1917.
Galinat, W. C. (1959). The phytomer in relation to floral homologies in the American Maydea. *Bot. Mus. Lefl. Harvard Univ.* **19**, 1-32.
Gifford, E. M. and Foster, A. S. (1989). *Morphology and Evolution of Vascular Plants*. New York: W. H. Freeman.
Harrison, C. J. and Langdale, J. A. (2010). The developmental pattern of shoot apices in *Selaginella kraussiana* (Kunze) A. Braun. *Int. J. Plant Sci.* **171**, 690-692.
Harrison, C. J., Corley, S., Moylan, E., Alexander, D., Scotland, R. W. and Langdale, J. A. (2005). Independent recruitment of a conserved developmental mechanism during leaf evolution. *Nature* **434**, 509-514.
Harrison, C. J., Rezvani, M. and Langdale, J. A. (2007). Growth from two transient apical initials in the meristem of *Selaginella kraussiana*. *Development* **134**, 881-889.
Harrison, C. J., Roeder, A. H., Meyerowitz, E. M. and Langdale, J. A. (2009). Local cues and asymmetric cell divisions underpin body plan transitions in the moss *Physcomitrella patens*. *Curr. Biol.* **19**, 461-471.
Hill, J. (2001). Meristem development at the sporophyll pinna apex in *Ceratopteris richardii*. *Int. J. Plant Sci.* **16**, 235-247.
Hofmeister, W. (1857). Beitrage zur entwicklungsgeschichte der gefasskryptogamen. II. *Abh. Math. Phys. Cl. Königl. Sächs. Ges. Wiss.* **3**, 601-682.
Jones, C. S. and Drinnan, A. N. (2009). The developmental pattern of shoot apices in *Selaginella kraussiana* (Kunze) A. Braun. *Int. J. Plant Sci.* **170**, 1009-1018.
Kaplan, D. R. (1996). *Principles of Plant Morphology*. Berkeley, CA: Odin Readers.
Kenrick, P. and Crane, P. R. (1997). *The Origin and Early Diversification of Land Plants: A Cladistic Study*. London: Smithsonian Institution Press.
Kny, L. (1875). Die entwicklung der parkeriaceen, dargestellt an *Ceratopteris thalictriodes*. *Nova Acta Ksl. Leop. Carol. Deut. Akad. Natur.* **37**, 1-80.
Pray, T. R. (1960). Ontogeny of the open dichotomous venation in the pinna of the fern Nephrolepis. *Am. J. Bot.* **47**, 319-328.
Prigge, M. J. and Clarke, S. E. (2006). Evolution of the class III HD-Zip gene family in land plants. *Evol. Dev.* **8**, 350-361.
Pryer, K., Schuettpelz, E., Wolf, P., Schneider, H., Smith, A. and Cranfill, R. (2004). Phylogeny and evolution of ferns (monilophytes) with a focus on the early leptosporangiate divergences. *Am. J. Bot.* **91**, 1582-1598.
Richards, J. H., Zenk Beck, J. and Hirsch, A. M. (1983). Structural investigations of asexual reproduction in *Nephrolepis exaltata* and *Platycerium bifurcatum*. *Am. J. Bot.* **70**, 993-1001.
Sanders, H., Rothwell, G. and Wyatt, S. (2009). Key morphological alterations in the evolution of leaves. *Int. J. Plant Sci.* **170**, 860-868.
Sano, R., Juarez, C., Hass, B., Sakakibara, K., Ito, M., Banks, J. and Hasebe, M. (2005). *KNOX* homeobox genes potentially have similar function in both diploid unicellular and multicellular meristems, but not in haploid meristems. *Evol. Dev.* **7**, 69-78.
Steeves, T. A. and Sussex, I. M. (1989). *Patterns in Plant Development*. Cambridge: Cambridge University Press.
Steingraeber, D. A. and Fisher, J. B. (1986). Indeterminate growth of leaves in Guarea (Meliaceae): a twig analogue. *Am. J. Bot.* **73**, 852-862.
Tsiantis, M. and Hay, A. (2003). Comparative plant development: the time of the leaf? *Nat. Rev. Genet.* **4**, 169-180.
White, R. and Turner, M. (1995). Anatomy and development of the fern sporophyte. *Bot. Rev.* **61**, 281-305.
Zimmermann, W. (1952). Main results of the 'Telome Theory'. *Palaeobotanist* **1**, 456-470.

Table S1. Frequency of sector sizes found on 114 randomly selected fronds

Size of sector (number of pinnae)	Frequency
1	124
2	37
3	25
4	3
5	2
6	0
7	0
8	0
9	0
10	0

Table S2. Frequency predictions of sectors encompassing between one and four pinnae, for all the variants on models tested

Model	Number of pinnae	Order	Proportion with one pinna	Proportion with two pinnae	Proportion with three pinnae	Proportion with four pinnae	Proportion with five pinnae	Within confidence?	Difference
Observed			0.6458	0.1927	0.1302	0.0156	0.0104		
5A	2	N/A	0.6422	0.3362	0.0139	0.0073	0.0003	YNNYN	1.1032e+03
5A	4	N/A	0.6487	0.1728	0.0055	0.1618	0.0053	YYNNY	1.2758e+03
5B	2	N/A	0.6447	0.3335	0.0143	0.0068	0.0004	YNNYN	1.0485e+03
5B	3	N/A	0.6442	0.1218	0.2200	0.0076	0.0022	YNNYN	5.2456e+02
5B	4	N/A	0.6508	0.0913	0.0824	0.1642	0.0055	YNNNY	1.3241e+03
5C	2	N/A	0.6901	0.2904	0.0134	0.0055	0.0005	YNNNN	7.5779e+02
5C	3	N/A	0.6796	0.1102	0.1969	0.0078	0.0078	YNNYN	4.7624e+02
5C	4	N/A	0.6745	0.0864	0.0795	0.1487	0.0059	YNNNY	1.2188e+03
5D	2	P+R	0.6495	0.3298	0.0129	0.0073	0.0003	YNNYN	1.0264e+03
5D	3	P+R	0.5431	0.2274	0.2143	0.0071	0.0038	NYNYY	8.5583e+02
5D	4	P+R	0.4880	0.1688	0.1704	0.1614	0.0045	NYYNY	2.0943e+03
5D	2	R+P	0.4876	0.4838	0.0134	0.0142	0.0005	NNNYN	4.4886e+03
5D	3	R+P	0.4290	0.2240	0.3277	0.0069	0.0048	NYNYY	3.4364e+03
5D	4	R+P	0.4118	0.1673	0.1641	0.2403	0.0046	NYYNY	4.3022e+03
5E	2	P+R	0.6495	0.3300	0.0135	0.0065	0.0002	YNNYN	1.0092e+03
5E	3	P+R	0.5338	0.2317	0.2193	0.0066	0.0042	NYNYY	9.7736e+02
5E	4	P+R	0.4852	0.1709	0.1694	0.1628	0.0045	NYYNY	2.1874e+03
5E	2	R+P	0.5551	0.4199	0.0137	0.0107	0.0005	NNNYN	2.5488e+03
5E	3	R+P	0.4893	0.2037	0.2891	0.0082	0.0040	NYNYY	2.0125e+03
5E	4	R+P	0.4528	0.1532	0.1556	0.2230	0.0052	NYYNY	3.4266e+03
5B + 2	3	N/A	0.7263	0.0991	0.1637	0.0071	0.0013	NNYYN	5.8604e+02
5D + 1	3	P+R	0.6454	0.1771	0.1650	0.0071	0.0029	YYYYN	1.3536e+02
5D + 1	3	R+P	0.5663	0.1754	0.2430	0.0075	0.0031	NYNYY	5.8604e+02

Columns show the model of cell division corresponding to diagrams in Fig. 5. For examination of whether later divisions of final products shown in Fig. 5B,D occur, additional numbers of cell divisions are denoted in the last three rows.

'Number of pinnae', final number of pinnae set to arise from each merophyte; 'Order', the order of specification of cells becoming pinnae and rachis segments; 'P+R', pinna specified first; 'R+P', rachis specified first; proportion with one to five pinnae, the proportionate frequency of sectors expected under the set parameters; 'Within confidence?', statements of whether the observed data fall within 95% confidence intervals of the predictions for each sector size; Y, yes; N, no; 'Difference', total sum of the squared difference between predicted and observed data for all sector sizes.